Author/s:
Rosas, HD;Chen, YI;Doros, G;Salat, DH;Chen, NK;Kwong, KK;Bush, A;Fox, J;Hersch, SM

Title:
Alterations in brain transition metals in Huntington disease: An evolving and intricate story

Date:
2012-07-01

Citation:
Rosas, H. D., Chen, Y. I., Doros, G., Salat, D. H., Chen, N. K., Kwong, K. K., Bush, A., Fox, J. & Hersch, S. M. (2012). Alterations in brain transition metals in Huntington disease: An evolving and intricate story. Archives of Neurology, 69 (7), pp.887-893. https://doi.org/10.1001/archneurol.2011.2945.

ONLINE FIRST

Alterations in Brain Transition Metals in Huntington Disease

An Evolving and Intricate Story

H. Diana Rosas, MD; Y. Iris Chen, PhD; Gheorghe Doros, PhD; David H. Salat, PhD; Nan-kuei Chen, PhD; Ken K. Kwong, PhD; Ashley Bush, MD, PhD; Jonathan Fox, PhD; Steven M. Hersch, MD, PhD

Background: Aberrant accumulation of transition metals in the brain may have an early and important role in the pathogenesis of several neurodegenerative disorders, including Huntington disease (HD).

Objective: To comprehensively evaluate and validate the distribution of metal deposition in the brain using advanced magnetic resonance imaging methods from the premanifest through symptomatic stages of HD.

Design: Observational study.

Setting: University imaging center.

Participants: Twenty-eight HD expanded gene carriers, 34 patients with symptomatic HD, and 56 age- and sex-matched healthy control subjects were included in the study.

Interventions: Participants underwent magnetic resonance imaging for the quantification of the phase evolution of susceptibility-weighted images.

Main Outcome Measures: To verify the identity of the metals responsible for the changes in the phase evolution of the susceptibility signal in the brain and to assess correlations with systemic levels. Inductively coupled plasma mass spectrometry was used to measure transition metal concentrations in postmortem brains.

Results: In the basal ganglia, progressive increases in the phase evolution were found in HD, beginning in premanifest individuals who were far from expected onset and increasing with proximity to expected onset and thereafter. Increases in the cerebral cortex were regionally selective and present only in symptomatic HD. Increases were verified by excessive deposition of brain iron, but a complex alteration in other transition metals was found.

Conclusion: An important and early role of altered metal homeostasis is suggested in the pathogenesis of HD.

Arch Neurol. Published online March 5, 2012.
doi:10.1001/archneurol.2011.2945

HUNTINGTON DISEASE (HD) is a progressive neurodegenerative disorder that causes severe cognitive, motor, and psychiatric disturbances. The genetic basis is an unstable expansion of a triplet repeat that codes for glutamine in the N-terminus of the protein huntingtin, which is widely expressed throughout the body. Transition metals, particularly iron and copper, have been implicated in the pathogenesis of HD. Iron is a potent cause of oxidative damage, which has long been known to accompany neurodegeneration in HD.[1] Copper directly catalyzes the oxidation and cysteine cross-linking of huntingtin and may be essential for the oligomerization process that promotes the toxic effects of the mutant protein, while reducing its clearance.[2] Evidence has shown that iron and copper concentrations are elevated in the forebrain of HD transgenic mice, and results of human postmortem and magnetic resonance (MR) imaging investigations have demonstrated elevations of iron and copper in the atrophic basal ganglia in symptomatic and advanced HD.[3,4] The metal-binding protein clioquinol is neuroprotective in cellular and mouse models of HD, indicating that metal modulation has significant therapeutic potential.[5] However, alterations in iron and copper levels, as well as in other transition metals, during the course of HD remain poorly understood.

Although other researchers[3,4] have shown changes in traditional measures of susceptibility-weighted imaging in patients with symptomatic HD, it is unknown whether brain metal accumulation might start early enough to contribute to pathologic conditions during the premanifest period (pre-HD). Our hypoth-

Author Affiliations are listed at the end of this article.

esis was that alterations in metal deposition occur early before symptoms occur and may have a significant role in the conversion from health to disease. In the present study, we sought to more extensively evaluate changes in transition metals in HD, starting with pre-HD through early to middle stages of HD. We used a novel MR analytical method that takes advantage of changes in the field map (FM) from the phase evolution of the susceptibility-weighted imaging signal to measure changes in paramagnetic metal content throughout the brain. To verify the identity of the transition metals measured by MR imaging, we also used inductively coupled plasma mass spectrometry to measure them directly in postmortem tissue from patients with HD.

METHODS

PARTICIPANTS

Included in the study were the following 3 groups of participants: (1) Twenty-eight (15 male and 13 female) premanifest HD expanded gene carriers (pre-HD group), with a mean (SD) age at study enrollment of 44.0 (10.3) years, a mean (SD) estimated time to onset of 14.0 (8.1) years at study enrollment, and a mean (SD) CAG triplet repeat length of 41.6 (1.5). (2) Thirty-four (17 male and 17 female) patients with symptomatic HD (HD group), spanning clinical stage 1 to stage 3, with a mean (SD) age at study enrollment of 52.1 (10.7) years and a mean (SD) CAG triplet repeat length of 44.1 (3.2). (3) Fifty-six (21 male and 35 female) age- and sex-matched healthy control participants, with a mean (SD) age at study enrollment of 48.0 (14.6) years. Several participants underwent second imaging more than 6 months apart. Analyses performed that excluded second imaging results led to similar results, indicating that these could be treated as independent measures. Therefore, a total of 162 images were analyzed: 36 from the pre-HD group, 65 from the HD group, and 61 from the control group. Volunteers in the pre-HD and HD groups were recruited through the HD clinic at Massachusetts General Hospital, Boston. Procedures were explained, and consent was obtained according to the Declaration of Helsinki. Study protocols were approved by the Massachusetts General Hospital Internal Review Board. Patients with symptomatic HD had unequivocal motor symptoms and a known trinucleotide repeat expansion; individuals with pre-HD had a known trinucleotide repeat expansion but did not have symptoms. All participants were evaluated by one of us with expertise in HD (H.D.R.).[6]

MR IMAGING

Magnetic resonance imaging was performed using a 1.5-T system (Avanto; Siemens) equipped with a 12-channel receiver head matrix coil at the Massachusetts General Hospital Athinoula A. Martinos Center for Biomedical Imaging. Two sets of 3-dimensional, magnetization-prepared, rapid gradient-echo imaging data were acquired for each participant using the following variables: echo time of 3.31 milliseconds, repetition time of 2730 milliseconds, flip angle of 7°, field of view of 256 mm, pixel matrix of 256 × 171, and sagittal section thickness of 1.33 mm for anatomical analyses. A multiecho gradient–weighted sequence was used to acquire multi–echo time data using the following variables: repetition time of milliseconds, 32 echoes, echo time of 2 to 40.75 milliseconds at a 1.25-millisecond step, voxel size and later echoes at 1.25-millisecond increments, and 72 sagittal sections with spatial resolution of $2 \times 2 \times 2$ mm^3. Artifacts in the susceptibility maps were avoided by using the first echo data only to determine phase reliability and to mask brain tissue.

FIELD MAPPING EVOLUTION MEASUREMENTS

Field mapping was performed using software (MATLAB; MathWorks) developed in-house. First, B_0 magnetic FM values were calculated from odd echoes of the acquired multi–echo time data by linearly fitting the phase evolution over time after unwrapping the phase values.[7] Note that the calculated FM values include contributions from microscopic susceptibility field gradients (eg, resulting from local metal accumulation) and from macroscopic susceptibility field gradients (eg, created by air-tissue interfaces). To reveal only the microscopic susceptibility–induced FM values, the macroscopic susceptibility–induced field gradients were mathematically removed using a procedure similar to the high-pass filtering used in susceptibility-weighted imaging.[8,9] Specifically, the B_0 magnetic FM values were spatially smoothed (reflecting the macroscopic field gradients that are slowly varying in space) using the csaps function built in MATLAB[9] and then subtracted from the original B_0 magnetic FM values. The output data were microscopic susceptibility–dominant B_0 magnetic FM values, reflecting the metal-induced field changes for each voxel.

Phase images were obtained after combining the multichannel data using a uniform sensitivity algorithm. Phase aliasing and spatial wraparound artifact were resolved with a spatial unwrapping using available software (PRELUDE function from FSL; http://www.fmrib.ox.ac.uk/fsl/fsl/other.html). To remove varying contributions from radio frequency inhomogeneity, polynomials were fitted and subsequently subtracted to decrease noise. Air-tissue susceptibility artifacts were removed using the csaps function (smoothing of 0.4).[10] Voxels with an absolute value exceeding 1000 Hz were considered not reliable. The magnitude of the odd echoes was chosen to reduce signal dropout due to intravoxel spin dephasing. Field map values were subsequently calculated by a linear fitting of the phase evolution against echo time values for each voxel.

BRAIN COREGISTRATION AND REGION-OF-INTEREST SEGMENTATION

The image-processing methods used (FreeSurfer 4.5; http://surfer.nmr.mgh.harvard.edu/pub/dist/freesurfer/4.5.0/) have been previously described in detail.[11,12] For correlational analyses, an automated parcellation scheme was used,[13] and the mean cortical thickness was calculated as previously noted.[14] Each individual FM was coregistered with the corresponding participant's T1-weighted anatomical images.

REGIONAL POSTMORTEM BRAIN ANALYSES

To further elucidate the changes in transition metals in HD indicated by neuroimaging, iron, manganese, zinc, and copper concentrations were obtained from brain regions, including the pallidum, putamen, anterior frontal, precentral, anterior cingulate, and occipital cortex, from 25 (10 female and 15 male) HD postmortem brains (mean [SD] age of 58.6 [2.5] years, with 9 Vonsattel and DiFiglia[15] grade 1 or 2 and 16 grade 3 or 4) and from 12 (7 female and 5 male) healthy controls (mean [SD] age of 61.9 [3.6] years). All samples were dissected by Jean-Paul Vonsattel, MD (Massachusetts General Hospital) and were obtained from the Alzheimer Disease Research Center at Massachusetts General Hospital (HD pallidum, control, and HD putamen), the Harvard Brain Bank at McLean Hospital (control pallidum), or the New York Brain Bank at Columbia Univer-

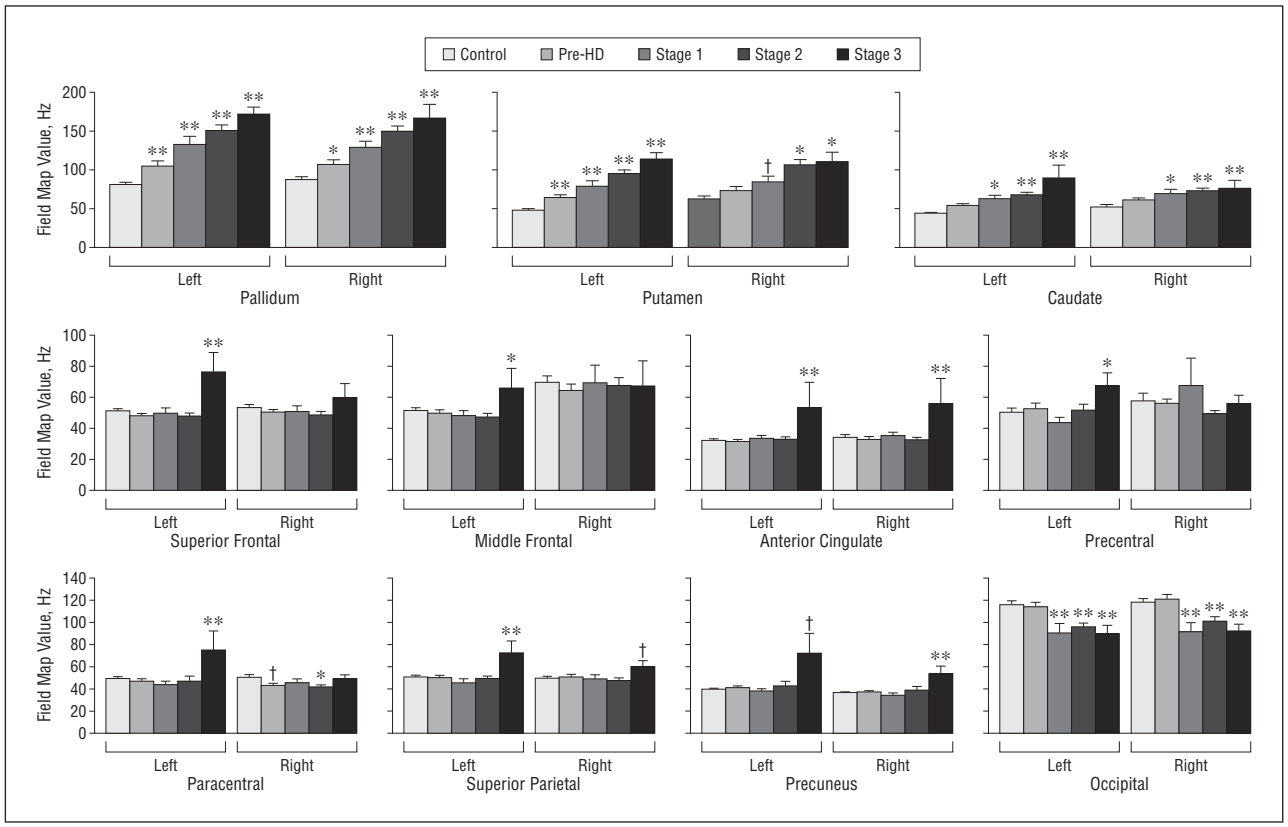

Figure 1. Field map values by clinical stage. Field map values were significantly higher in striatal structures, beginning in the premanifest period of Huntington disease (pre-HD), in the pallidum and putamen, and in several cortical structures, primarily in patients with more advanced disease, suggesting regionally and temporally distinct accumulation of metals in the brain in Huntington disease. †$P>.05$ but $<.01$. *$P>.01$ but $\leq.05$. **$P\leq.01$.

sity in New York City (HD and control cortex and HD pallidum). Postmortem procurement intervals were less than 4 hours. Grade 2 according to Vonsattel and DiFiglia[15] would roughly correspond to HD clinical stage 2 or 3. There was insufficient caudate in the HD cohort for adequate evaluation. Brain samples were homogenized in 30 volumes of binding buffer containing protease inhibitor and were subsequently applied directly to copper-charged columns (HiTrap Chelating Sepharose; Amersham) as previously described.[16]

STATISTICAL ANALYSIS

To study the relationship between the FM value distributions and the main risk groups (pre-HD, HD, and control), we used 1-way analysis of variance *F* test. Images from patients with HD were also stratified by clinical stage to evaluate a potential relationship between FM value and disease severity. Results were adjusted for multiple comparisons using the method by Dunnett.[17]

For the postmortem analyses, differences in the regional concentrations between the HD and control groups were evaluated using 2-sided *t* test. Uncorrected results are presented. Significance was set at $P\leq.05$, and $P<.10$ represented notable trends that deserve further careful evaluation. All statistical analyses were performed using available software (R; http://www.R-project.org).[18]

RESULTS

Our results suggest that metal dysregulation, supported by the aberrant regionally selective deposition throughout the brain, may contribute to the pathogenesis of HD. These findings imply that metal modulation is a potential target for neuroprotection and support the conjecture that measurement of metals in the brain by MR imaging could provide useful markers of HD progression and response to treatments.

FM VALUES

As shown in **Figure 1**, the mean FM values in the pre-HD and HD groups were significantly higher than those in the control group in the basal ganglia structures, including bilaterally in the caudate ($P=.001$), putamen ($P<.001$), and globus pallidus ($P<.001$), starting with pre-HD. Also shown was a trend for higher FM values with increasing disease severity, starting with significant increases in pre-HD. In contrast, FM values were not significantly different in the pre-HD or HD groups compared with the control in the thalamus, hippocampus, or amygdala.

In the cortex, several regions demonstrated higher FM values in the HD group, but values reached significance only in stage 3, representing patients with the most advanced stage of disease studied. The regions with the greatest FM values included the following: left superior frontal ($P<.001$), left middle frontal ($P=.03$), left and right anterior cingulate ($P=.008$ and $P=.004$, respectively), left and right paracentral ($P=.03$ and $P=.004$, respectively), left and right precuneus ($P<.001$ and $P=.001$, respec-

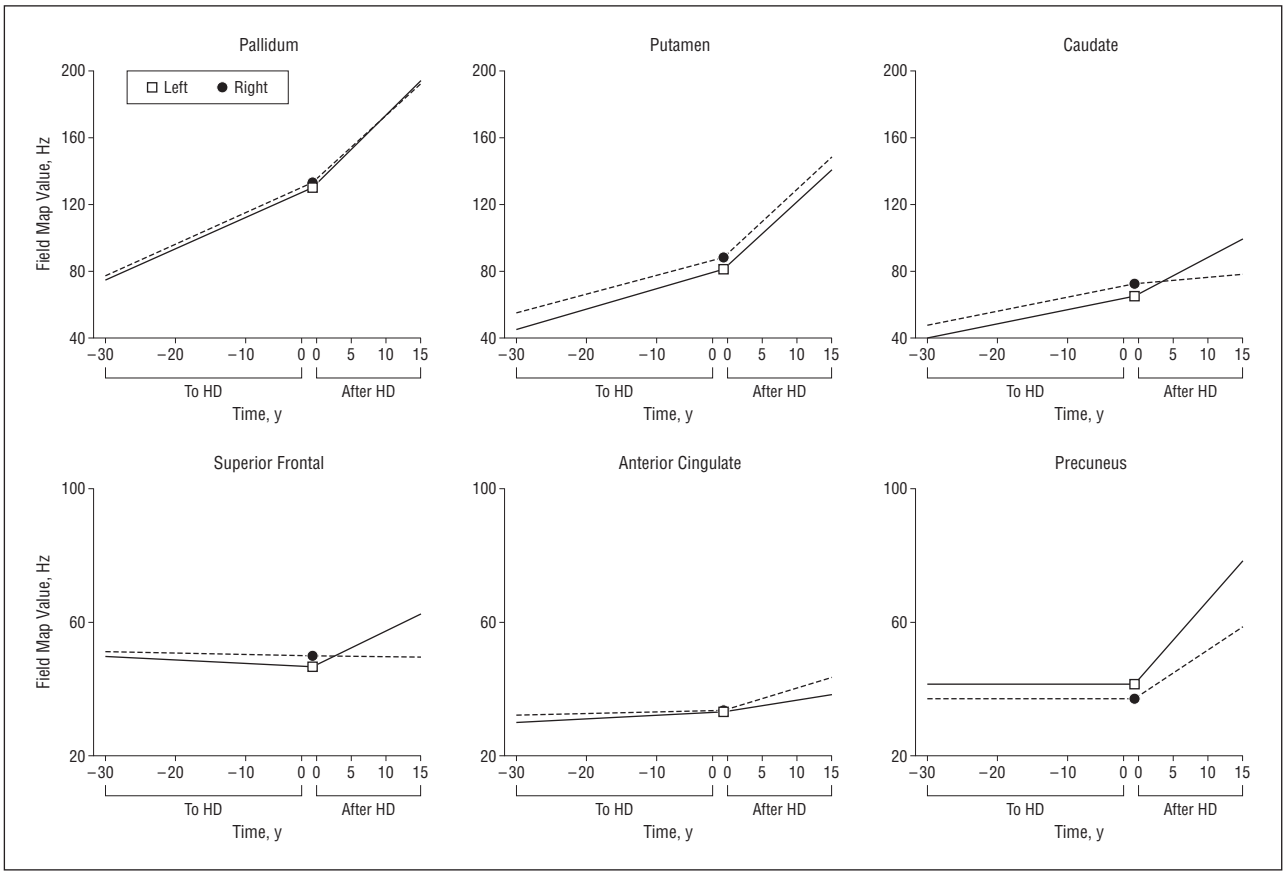

Figure 2. Progression models. Using expected time to Huntington disease (HD) onset, we found significant increases in the rate of field map value increases in the basal ganglia in the premanifest period of Huntington disease (pre-HD); the slope was steeper after diagnosis. Cortical field map value increases were present only after diagnosis, supporting an early important role of alterations in metals in HD.

tively), right cuneus ($P=.04$), and left precentral ($P=.04$). No significant increases were noted in other cortical regions, including the cuneus, precuneus, and regions of temporal cortex, suggesting a regionally selective process.

RELATIONSHIP BETWEEN FM VALUE AND DISEASE SEVERITY

Based on the Total Functional Capacity Scale (TFC), the standard measure of HD progression used in clinical research, the rate of functional decline is 0.72 U per year.[19] We modeled FM values as a function of disease progression using each change in 0.72 U on the TFC as an estimate of approximately 1 year of symptomatic disease; in this way, we developed a model of progression starting from expected time to onset to estimated time from onset. Selected associations between FM value and disease severity are shown in **Figure 2**.

After adjusting for age, we found a significant association between FM value and CAG triplet repeat length, but not TFC score, bilaterally in the caudate, accumbens, putamen, pallidum, and anterior cingulate. Other significant associations between FM value and TFC score were found in the left superior parietal ($P=.010$), left middle frontal ($P=.019$), left thalamus ($P=.038$), left superior frontal ($P=.043$), right inferior parietal ($P=.078$), and left precentral ($P>.10$). A significant increase in FM value was associated with estimated expected onset (in years), based on the model by Langbehn et al,[20] in the pre-HD group bilaterally in the caudate, left putamen, paracentral, and pallidum and in the left anterior cingulate ($P=.02$).

Our age-prediction models demonstrated that FM increases in the pre-HD and HD groups in basal ganglia structures and in cortical regions exceed increases that might be due to age, as shown in eFigure 1 (http://www.archneurol.com). The green line represents the mean values observed in the control group, and the gray line represents the 95% upper bounds of age-related prediction values. Therefore, FM values falling above the solid green line represent values greater than expected for age; FM values falling above the gray line exceed the 95% prediction limit and are significantly higher than expected for age. Values for the pre-HD group are given in blue and those for the HD group in red. In the left caudate, more than 81% of the individual pre-HD FM values fell above this limit ($P<.0001$). In the left putamen, more than 95% of the individual pre-HD FM values fell above this limit. This was more apparent in the HD group, suggesting an acceleration of increases in FM values, with disease exceeding that expected for age.

Age-predicted models for cortical regions of interest are not shown. However, in several cortical regions, including the left anterior cingulate ($P=.001$), left precentral ($P=.005$), left superior frontal ($P=.02$), right middle frontal ($P=.04$), right pericalcarine ($P=.04$), and right pre-

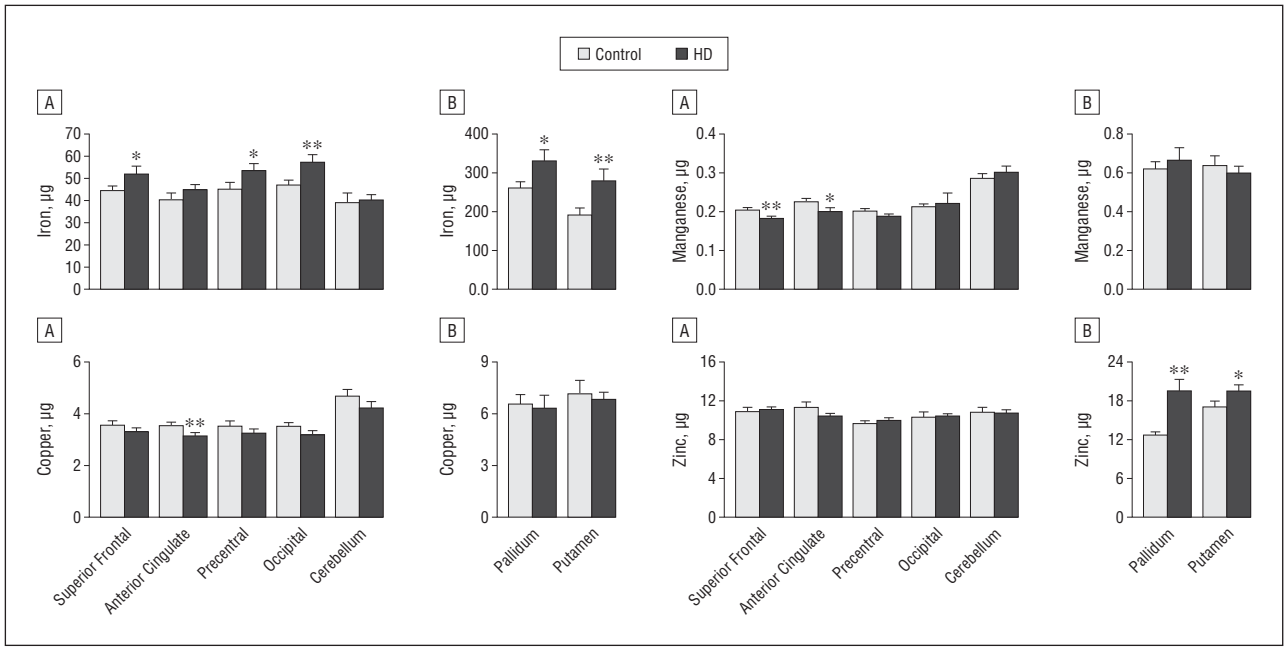

Figure 3. Characterization of metal concentrations ex vivo. Significant increases in iron were present in the basal ganglia and in several cortical structures. In contrast, significant decreases in cortical copper and manganese were observed in Huntington disease (HD), suggesting complex dynamics. Data for cortical regions (A) and subcortical regions (B) are displayed. Bars extend 1 SE. Micrograms are per gram of wet weight. *$P<.01$. **$P\leq.05$.

cuneus ($P=.02$), FM values were greater than the 95% prediction limit, supporting early disease-specific changes in iron deposition.

POSTMORTEM BRAIN ANALYSES

Significant increases in iron concentrations were present in HD postmortem brains in several regions, shown in **Figure 3**, including the putamen, pallidum, and occipital cortex, with a trend for higher iron concentrations in the superior frontal and precentral regions but with no significant differences in the anterior cingulate or cerebellum. Significant increases in iron concentrations in these structures were present starting in Vonsattel and DiFiglia[15] grades 1 to 2, shown in eFigure 2, suggesting an important early role of these changes in selective cortical vulnerability. Zinc concentrations were also significantly higher in the pallidum, with a trend for higher concentrations in the putamen, but there were no differences in zinc concentrations in the cortical regions sampled. Paradoxically, manganese concentrations were significantly lower in the superior frontal region, with a trend for lower concentrations in the anterior cingulate in the HD group.

COMMENT

We combined in vivo and ex vivo approaches to characterize and validate alterations in metal deposition that occur in the brain in HD; our findings suggest a complex alteration in metal homeostasis that may have profound clinical implications not only for HD but also for other neurodegenerative disorders. Using MR imaging, we found that concentrations of paramagnetic metals were elevated in pre-HD, long before the presence of clinical symptoms, but were distributed in a regionally selective pattern that recapitulates the neuropathology of HD. Indeed, the progressive regional increases in the MR imaging signal corresponded to those suggested previously, namely, the basal ganglia and cortex, including the sensorimotor, parietal, and occipital regions.[21] The most significant cortical elevations were present in stage 3 HD, in which motor and cognitive symptoms are generally prominent but patients remain ambulatory and independent for many activities of daily living. The ex vivo work using inductively coupled plasma mass spectrometry confirms that these increases correspond to aberrant regional iron deposition in the brain in HD.

Iron, stored within ferritin, is thought to provide most of the paramagnetic metal signal in the brain; however, copper and manganese could also have contributed to our findings if they are sufficiently altered as well. Although ferritin is a storage form of iron, its increase suggests greater availability to do damage through some combination of more transport of iron into the brain, reduced efflux from cells, or redistribution from other compartments (ie, alteration of brain homeostasis). In addition to ferritin, iron is present in the brain, bound to various transporters, and is a cofactor for many metalloproteins.[22] In its ferrous form, it can react with hydrogen peroxide (produced by mitochondria) and molecular oxygen to produce hydroxyl radicals (Fenton reaction). Hydroxyl radicals can further release iron (II) from iron-sulfur centers and other iron-containing compounds, promoting greater oxidative stress and perhaps further increasing the MR imaging signal if ferritin increases as a result. Any increase in the exposure of iron to cellular biomolecules could readily potentiate neurodegeneration, and indeed there is extensive evidence for early and profound oxidative damage to proteins, lipids, and nucleic acids in the HD brain.[1] Even small metal el-

evations greatly increase cellular oxidative stress through redox reactions,[23] have negative consequences for energy metabolism,[24] and may affect signal transduction and gene transcription[25] and result in DNA damage and eventually cell death.

At the cellular level, iron (ferritin) is predominantly stored in oligodendroglia in the brain but is also significantly present in microglia, astroglia, and neurons, each of which contain iron transport and storage systems. Increases that we have detected may or may not be pancellular depending on the underlying cause of the iron increase. Notably, the density of oligodendroglia is elevated in the HD brain,[26] even from individuals with pre-HD,[27] and it is possible that oligodendrogliosis contributes to the increase in FM values. The early aberrant accumulation of iron in the basal ganglia suggests that iron-induced oxidative stress, as well as altered regulation of iron-dependent enzymes, could have an important role in the early selective vulnerability of the basal ganglia during pre-HD.

Copper has been previously reported to be elevated in human HD postmortem putamen[28] but not in other brain regions. It has also been reported to be increased in the R6/2 transgenic mouse model of HD but not in the CAG140 knockin model.[11] In the present study, we did not detect increased copper in the human brain. Zinc was increased in the putamen and pallidum; however, it is a diamagnetic metal and is unlikely to contribute significantly to the FM signal. Notably, manganese was decreased in the cortex, perhaps because of depletion of the antioxidant manganese superoxide dismutase or displacement by iron of its transport by transferrin.

Modeling of the MR imaging data using a predictive formula for time to HD onset in individuals in the pre-HD group and for clinical progression in the HD group, as defined by the TFC, demonstrated the gradual accumulation of paramagnetic metals in the basoganglia as patients neared onset, followed by an apparent accelerated accumulation after clinical diagnosis. Notably, the DNA damage marker 8-hydroxy-2-deoxyguanosine, which is released from the brain in HD into the circulation and urine,[29] is detected at low levels in pre-HD and at much higher levels once symptoms have manifested,[30] a possible molecular correlate of oxidative damage that may be caused by accumulating metals. The upward inflection in both of these markers might indicate the onset of clinical disease.

In summary, our findings indicate that metal homeostasis is disturbed in HD, as measured by MR imaging and validated in postmortem brain. These results implicate metals as potential therapeutic targets and suggest that measurement of metals by MR imaging could provide useful markers of HD progression and response to treatment. Detailed examination of metal absorption, transport, and storage mechanisms, as well as the regulation of the metalloproteins that use metals, will be necessary to fully understand these findings.

Accepted for Publication: October 27, 2011.
Published Online: March 5, 2012. doi:10.1001/archneurol.2011.2945

Author Affiliations: Departments of Neurology (Drs Rosas and Hersch) and Radiology (Dr Salat), Center for Neuroimaging of Aging and Neurodegenerative Diseases (Drs Rosas and Salat), MassGeneral Institute for Neurodegeneration (Drs Rosas, Fox, and Hersch), and Athinoula A. Martinos Center for Biomedical Imaging (Drs Y. I. Chen, Salat, and Kwong), Massachusetts General Hospital and Harvard Medical School, and Department of Biostatistics, Boston University (Dr Doros), Boston; Brain Imaging and Analysis Center, Duke University, Durham, North Carolina (Dr N.-k. Chen); Oxidation Biology Laboratory, Mental Health Research Institute, University of Melbourne, Victoria, Australia (Dr Bush); and Department of Veterinary Sciences, University of Wyoming, Laramie (Dr Fox).
Correspondence: H. Diana Rosas, MD, Center for Neuroimaging of Aging and Neurodegenerative Diseases, Massachusetts General Hospital and Harvard Medical School, 149 13th St, Room 2275, Charlestown, MA 02129 (rosas@helix.mgh.harvard.edu).
Author Contributions: Drs Rosas and Y. I. Chen contributed equally to this work. Dr Salat performed most of the statistical analyses. *Study concept and design:* Rosas, Y. I. Chen, Salat, Kwong, and Hersch. *Acquisition of data:* Rosas, Salat, Fox, and Hersch. *Analysis and interpretation of data:* Rosas, Y. I. Chen, Doros, N.-k. Chen, Kwong, and Hersch. *Drafting of the manuscript:* Rosas, Y. I. Chen, Doros, N.-k. Chen, and Hersch. *Critical revision of the manuscript for important intellectual content:* Rosas, Y. I. Chen, Doros, Salat, N.-k. Chen, Kwong, Fox, and Hersch. *Statistical analysis:* Rosas, Y. I. Chen, Doros, and Fox. *Obtained funding:* Rosas and Hersch. *Administrative, technical, and material support:* N.-k. Chen, Kwong, Bush, and Hersch. *Study supervision:* Rosas, Salat, N.-k. Chen, and Hersch.
Financial Disclosure: None reported.
Funding/Support: This research was supported in part by the National Institutes of Health, including the following grants: R01NS042861 and NS058793 from the National Institute for Neurological Disorders and Stroke (Drs Rosas, Y. I. Chen, Doros, Salat, and Hersch), AT000613 (Drs Rosas, Y. I. Chen, and Hersch) and P01AT002048 from the National Institute of Biomedical Imaging and Bioengineering (Dr Kwong), R21EB005690 from the National Center for Complementary and Alternative Medicine (Dr N.-k. Chen), HDSA Coalition for the CURE (Dr Fox), FD003359 from the Food and Drug Administration (Drs Rosas, Y. I. Chen, and Hersch), SFCA07-101 from the International Foundation for Gastrointestinal Disorders, NR010827 from the National Institute of Nursing Research (Dr Salat), and National Health and Medical Research Council (Dr Bush).
Online-Only Material: The eFigures are available at http://www.archneurol.com.
Additional Contributions: Alex Bender, BA; Keith Malarick, BA; and Susan Maya, BA, helped in recruiting study participants, and Tyler Triggs, BA, and Stephanie Lee, BA, provided technical assistance. We are grateful to our patients and family members who so generously contributed their time and energy to this work, without whom it would not have been possible.

REFERENCES

1. Browne SE, Ferrante RJ, Beal MF. Oxidative stress in Huntington's disease. *Brain Pathol*. 1999;9(1):147-163.
2. Fox JH, Connor T, Stiles M, et al. Cysteine oxidation within N-terminal mutant huntingtin promotes oligomerization and delays clearance of soluble protein. *J Biol Chem*. 2011;286(20):18320-18330.
3. Bartzokis G, Lu PH, Tishler TA, et al. Myelin breakdown and iron changes in Huntington's disease: pathogenesis and treatment implications. *Neurochem Res*. 2007; 32(10):1655-1664.
4. Bartzokis G, Tishler TA. MRI evaluation of basal ganglia ferritin iron and neurotoxicity in Alzheimer's and Huntingon's disease. *Cell Mol Biol (Noisy-le-grand)*. 2000;46(4):821-833.
5. Nguyen T, Hamby A, Massa SM. Clioquinol down-regulates mutant huntingtin expression in vitro and mitigates pathology in a Huntington's disease mouse model. *Proc Natl Acad Sci U S A*. 2005;102(33):11840-11845.
6. Huntington Study Group. Unified Huntington's Disease Rating Scale: reliability and consistency. *Mov Disord*. 1996;11(2):136-142.
7. Reber PJ, Wong EC, Buxton RB, Frank LR. Correction of off resonance-related distortion in echo-planar imaging using EPI-based field maps. *Magn Reson Med*. 1998;39(2):328-330.
8. Rauscher A, Sedlacik J, Barth M, Mentzel HJ, Reichenbach JR. Magnetic susceptibility-weighted MR phase imaging of the human brain. *AJNR Am J Neuroradiol*. 2005;26(4):736-742.
9. Young GS, Feng F, Shen H, Chen NK. Susceptibility-enhanced 3-Tesla T1-weighted spoiled gradient echo of the midbrain nuclei for guidance of deep brain stimulation implantation. *Neurosurgery*. 2009;65(4):809-815.
10. Chen NK, Oshio K, Panych LP. Application of k-space energy spectrum analysis to susceptibility field mapping and distortion correction in gradient-echo EPI. *Neuroimage*. 2006;31(2):609-622.
11. Salat DH, Buckner RL, Snyder AZ, et al. Thinning of the cerebral cortex in aging. *Cereb Cortex*. 2004;14(7):721-730.
12. Fischl B, Liu A, Dale AM. Automated manifold surgery: constructing geometrically accurate and topologically correct models of the human cerebral cortex. *IEEE Trans Med Imaging*. 2001;20(1):70-80.
13. Desikan RS, Ségonne F, Fischl B, et al. An automated labeling system for subdividing the human cerebral cortex on MRI scans into gyral based regions of interest. *Neuroimage*. 2006;31(3):968-980.
14. Rosas HD, Salat DH, Lee SY, et al. Cerebral cortex and the clinical expression of Huntington's disease: complexity and heterogeneity. *Brain*. 2008;131(pt 4): 1057-1068.
15. Vonsattel JP, DiFiglia M. Huntington disease. *J Neuropathol Exp Neurol*. 1998;57 (5):369-384.
16. Fox JH, Kama JA, Lieberman G, et al. Mechanisms of copper ion mediated Huntington's disease progression. *PLoS One*. 2007;2(3):e334. http://www.ncbi.nlm.nih.gov/pmc/articles/PMC1828629/?tool=pubmed. Accessed January 6, 2012.
17. Dunnett CW. A multiple comparisons procedure for comparing several treatments with a control. *J Am Stat Assoc*. 1955;50:1096-1121.
18. R Web site. The R project for statistical computing. http://www.R-project.org. Accessed January 6, 2012.
19. Marder K, Zhao H, Myers RH, et al; Huntington Study Group. Rate of functional decline in Huntington's disease. *Neurology*. 2000;54(2):452-458.
20. Langbehn DR, Brinkman RR, Falush D, Paulsen JS, Hayden MR; International Huntington's Disease Collaborative Group. A new model for prediction of the age of onset and penetrance for Huntington's disease based on CAG length. *Clin Genet*. 2004;65(4):267-277.
21. Rosas HD, Salat DH, Lee SY, Zaleta AK, Hevelone N, Hersch SM. Complexity and heterogeneity: what drives the ever-changing brain in Huntington's disease? *Ann N Y Acad Sci*. 2008;1147:196-205.
22. Andreini C, Bertini I, Cavallaro G, Holliday GL, Thornton JM. Metal-MACiE: a database of metals involved in biological catalysis. *Bioinformatics*. 2009;25(16): 2088-2089.
23. Deb S, Johnson EE, Robalinho-Teixeira RL, Wessling-Resnick M. Modulation of intracellular iron levels by oxidative stress implicates a novel role for iron in signal transduction. *Biometals*. 2009;22(5):855-862.
24. Benchoua A, Trioulier Y, Zala D, et al. Involvement of mitochondrial complex II defects in neuronal death produced by N-terminus fragment of mutated huntingtin. *Mol Biol Cell*. 2006;17(4):1652-1663.
25. Mattson MP. Metal-catalyzed disruption of membrane protein and lipid signaling in the pathogenesis of neurodegenerative disorders. *Ann N Y Acad Sci*. 2004; 1012:37-50.
26. Myers RH, Vonsattel JP, Paskevich PA, et al. Decreased neuronal and increased oligodendroglial densities in Huntington's disease caudate nucleus. *J Neuropathol Exp Neurol*. 1991;50(6):729-742.
27. Gómez-Tortosa E, MacDonald ME, Friend JC, et al. Quantitative neuropathological changes in presymptomatic Huntington's disease. *Ann Neurol*. 2001;49 (1):29-34.
28. Dexter DT, Jenner P, Schapira AH, Marsden CD; The Royal Kings and Queens Parkinson's Disease Research Group. Alterations in levels of iron, ferritin, and other trace metals in neurodegenerative diseases affecting the basal ganglia. *Ann Neurol*. 1992;32(suppl):S94-S100.
29. Bogdanov MB, Andreassen OA, Dedeoglu A, Ferrante RJ, Beal MF. Increased oxidative damage to DNA in a transgenic mouse model of Huntington's disease. *J Neurochem*. 2001;79(6):1246-1249.
30. Hersch SM, Rosas HD. Biomarkers to enable the development of neuroprotective therapies for Huntington's disease. In: Lo DC, Hughes RE, eds. *Neurobiology of Huntington's Disease Applications to Drug Discovery*. New York, NY: CRC Press Taylor & Francis Group; 2010.